

THE CRITERION OF CHOOSING THE PROPER SEEDING PARTICLES

J. Novotný*, L. Manoch**

Abstract: *This paper is focused on the problem of the ability of seeding particles to follow the flow field. One of the most important factors influencing the resultant accuracy of the measurement is using the proper seeding particles for feeding the flow when measuring by Particle Image Velocimetry method – PIV. The aim of the paper is to provide comprehensible instruction for choosing the proper type of seeding particles with regard to the flow characteristics and required measurement accuracy. The paper presents two methods with the help of which it is possible to determine the seeding particles' ability to follow the flow field. The first method is based on the direct calculation of the phase lag and amplitude ratio between the particle and the fluid. The calculation is based on solution of the BBO equation for spherical particle. The other method results from the calculation of the particle time response, which defines the maximum frequency of disturbances, which are to be followed by the particle. In the conclusion, the method of choosing the seeding particles is proposed, depending on the required measurement accuracy.*

Keywords: *PIV, seeding particles, BBO, accuracy*

1. Introduction

When measuring with the help of Particle Image Velocimetry the particle image shift in time Δt is measured. Instead of measuring the liquid velocity, the distance of the particles covered in Δt is measured. The resultant measurement accuracy is i.a. influenced by the seeding particles' ability to follow the flow field, by the method of calculating the resultant shift and by other parameters by the help of which it is possible to identify the quality of obtained signal. Quite a few of authors dealt with the signal quality influence on the resultant accuracy of the measurement by the PIV method in the past decade. The authors most often deal with the influence of particular parameters (particle density, particle size, gradient, measured shift) on the resultant PIV measurement accuracy. Much attention is given to the influence of particular algorithms by the help of which the correlation plane is calculated. This paper is focuses only on the influence of seeding particles' ability to follow the flow field. Different authors, concerned themselves on the problem in the past. Their articles solve the movement of the spherical particle in the flow field in dependence on the amplitude ratio (phase lag) and Stokes number. The authors' use of the diagrams and conclusions is limited to the sizes of the particles, no longer commonly used. The resolution of the diagrams presented by the authors mentioned above doesn't allow precise reading of the required values. This paper aims to remedy the shortcomings. The particle's ability to follow the fluid movement is influenced by the density ratio of the particle and the liquid, by the shape and size of the particle and fluid viscosity. If we want to deal with the description of particle displacement in the flow field it is necessary to describe the displacement by means of the motion equation. The spherical or eventually at least oval-shaped seeding particles are ideal for the PIV measurement. The seeding particle displacement will be further solved on condition that the particle is spherical. This assumption is not always fulfilled; especially the solid particles made from SiO₂ or Al₂O₃ do not fulfill the assumption, but this simplification is necessary and does not lower the quality of obtained data.

* Ing. Jan Novotný, Ph.D. : CTU in Prague Faculty of Mechanical Engineering Department of Fluid Dynamics and Thermodynamics, Technická 4; 166 07, Prague; CZ, e-mail: jan.novotny@fs.cvut.cz

** Ing. Lukáš Manoch: CTU in Prague Faculty of Mechanical Engineering Department of Fluid Dynamics and Thermodynamics, Technická 4; 166 07, Prague; CZ, e-mail: lukas.manoch@fs.cvut.cz

2. Solutions of the BBO equation

The movement of the spherical particle carried by the viscosity liquid was already described by Basset. The equation derived by Basset is commonly classified as BBO equation. The other authors also concerned with the spherical particle displacement in both steady and unsteady flow are Basset, Boussinesq and Oseen. BBO equation can be written down in the form:

Where:

$$m_p \frac{du_p}{dt} = \frac{18 \mu_F}{\rho_p d_p^2} m_p (u_F - u_p) - m_F \frac{Du_F}{Dt} + \frac{1}{2} m_F \left(\frac{Du_F}{Dt} - \frac{du_p}{dt} \right) + 9 \sqrt{\frac{\rho_F \mu_F}{\pi}} \frac{m_p}{\rho_p d_p} \int_{t_0}^t \frac{Du_F - du_p}{\sqrt{t - \tau}} d\tau + (m_p - m_F) g. \quad (1)$$

u_p is velocity of the particle

u_F is fluid velocity

m_p is particle mass

m_F is mass of the fluid at particle-volume

d_p is particle diameter

μ_F is fluid viscosity

ρ_p is particle density

The given equation is valid for these cases:

The size of the smallest vortices is several times bigger than the particle diameter;

The Reynold's number calculated from the particle diameter and from the difference between liquid and particle velocity is lower than 1.

The particles density in the liquid has to be low enough in order to prevent from interaction among the individual particles as well as to prevent the particles features from changing during the process of adding the particles to the fluid;

The turbulence is homogeneous.

Quite a few of authors have made a detailed analysis of the influence of the particular equation terms (1) and thus we will not deal with it. Hjermfeld solved the equation (1) for the course of liquid velocity u_F and particle velocity u_P expressed with the help of Fourier's integral:

$$u_p = \int_0^{\infty} (\sigma \cos \omega t + \varphi \sin \omega t) d\omega \quad (2)$$

$$u_F = \int_0^{\infty} (\zeta \cos \omega t + \lambda \sin \omega t) d\omega \quad (3)$$

The expression for the velocity of the particle is the solution of the equation (1). In the equation (4), the velocity of the particle is expressed with the help of the liquid movement whose phase is shifted within an angle β and the amplitude is increased or decreased η -times:

$$u_p = \int_0^{\infty} \eta \left[\begin{array}{l} (\zeta \cos(\omega t + \beta) + \\ \varphi \sin(\omega t + \beta)) \end{array} \right] d\omega \quad (4)$$

Where:

$$\eta = \sqrt{(1 + f_1)^2 + f_2^2} \quad (5)$$

$$\beta = \tan^{-1} \left[\frac{f_2}{1 + f_1} \right] \quad (6)$$

When introducing the particle and liquid density as $s = \sigma_p / \sigma_F$ and the non-dimensional Stokes number N_s defined according to:

$$N_s = \sqrt{\frac{\nu}{\omega D^2}} \quad (7)$$

Where:

ω is angular velocity corresponding to the maximum frequency of disturbances in flow,

ν is kinematic viscosity of flowing fluid,

D is size of the seeding particle.

it is possible to express the coefficients f_1 and f_2 as functions N_s , s and D , for more detail see. The dependence of the amplitude η and displacement angle β ratio on the Stokes number is mentioned by Hjelmfelt as well as Sommerfeld for several particle and liquid density ratios. The results of the equations solution, indicated by the authors, are unsatisfactory for most of the PIV measurements for two reasons. Either the authors mention fluid and particle density ratio within the range that is not used

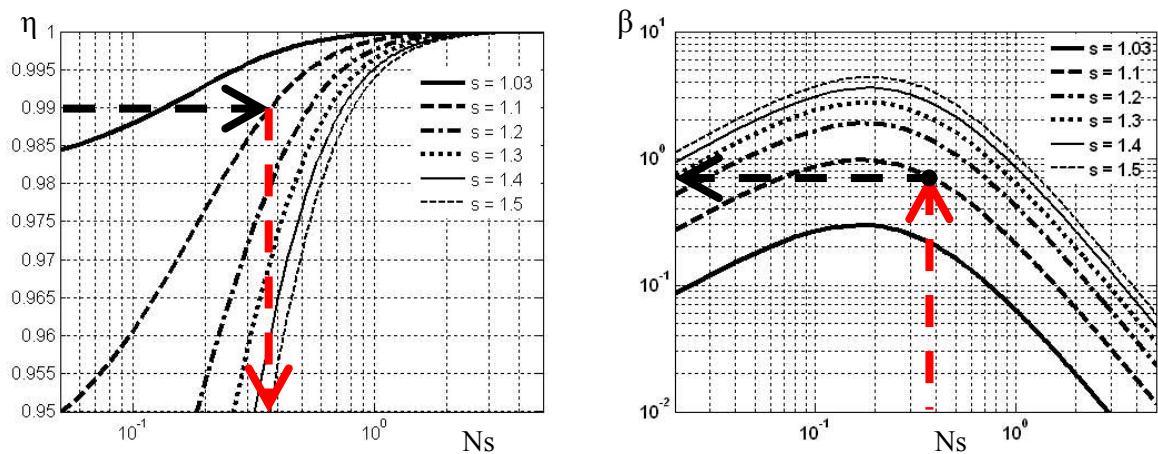


Fig. 1: Dependence of amplitudes ratio η and phase lag β on Stokes number N_s for particles flowing in water and for several values of density ratios

any longer at measuring by the PIV method [19], or they present the dependence of the phase lag (or actual and measured amplitude ratio) for the range of Stokes number obtained by PIV measurements very sporadically [40]. The resulting dependencies presented in those articles do not also meet the requirement for quick and precise determination of the range of application of different particle types, which are at the experimenter's disposal.

In order to generate the particular diagrams that enable to deduct the required data easily and quickly it is necessary to display the dependence of amplitudes ratio on Stokes number in the range of $0.95 < \eta < 1$. At this range it is possible to read easily the Stokes number by which the given particle moves with an amplitude deviation lower than one percent of the total velocity in the given place. It is necessary to consider different specific gravities of fluid and particle to make the presented dependencies complex. At measuring in liquids, the particle and liquid density ratios occur in the range of c. 1.03-1.5 (the difference between the particle and liquid density). Based on the solution presented by, it appears that if the particle density is identical to the liquid density then the difference in the phase lag and in the measured amplitude from the real liquid movement is zero. Such particles closely follow the liquid flow in case the characteristic disturbance size in the liquid is minimally several times bigger than the particle diameter. At measuring in the gases the density ratios s occur in the range from 20 for the expanded polystyrene micro balls up to the 2250 for Aluminum powder particles. For the measurement by the PIV method at low velocities, it is also possible to use helium bubbles that reach the density ratio s dependent on their size in the range of 0.9-1.1. The size of the particles generated in this manner is c. 1 mm and their application is limited to the very slow flow of the order of ones of meters per second. The Stokes number is used for transparent plotting of the phase lag against the amplitude ratio dependent on the fluctuation frequency in the flow. It is evident from the definition of the Stokes number that with increasing frequency the Stokes number decreases whereas with decreasing particle diameter the Stokes number increases. The dependencies of η and β

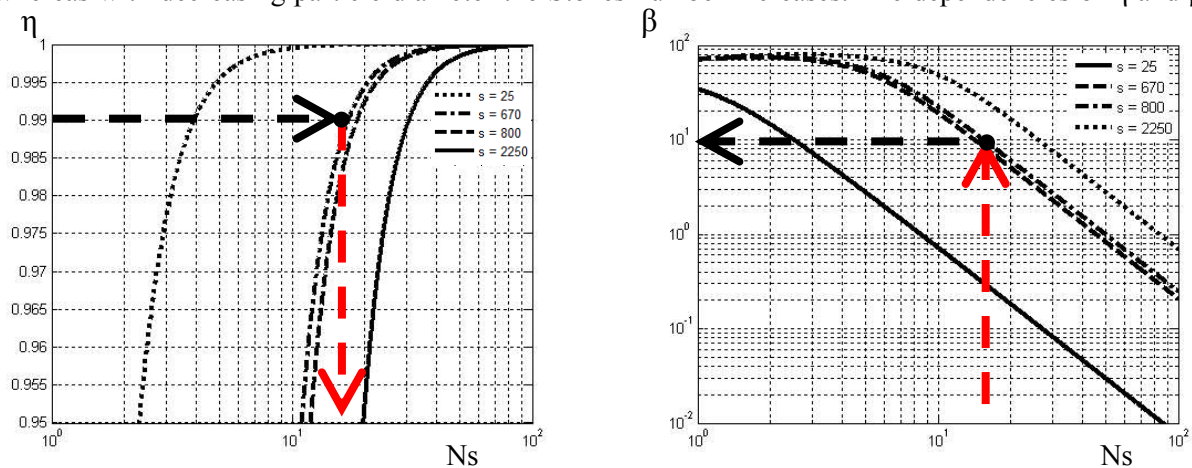


Fig. 2: Dependence of amplitudes ratio η and phase lag β on Stokes number N_s for particles flowing in air and for several values of density ratios.

on the Stokes number for the particular values of density ratio most frequent in the liquids and gases are displayed in the diagrams in Fig. 1 and 2.

3. Accuracy determination

The particle's ability to follow the flow field is shown in the diagrams in Fig. 1 to 4. It is possible to deduct the phase lag and particle and liquid amplitude ratio for the given frequency, and to read the particle and fluid density ratio. If we want to determine which particles are convenient for the existent experiment and which are not, it is necessary to determine the maximum frequency of disturbances which can be followed by the particles with given accuracy. For determination of the frequency that can be followed by the particles with the amplitude deviation lower than one percent ($\eta=0.99$) it is necessary to know:

- Mean value of particle diameter
- Specific density of particle and fluid
- Kinematic viscosity of fluid

It is possible to resume the determination of maximum frequency that can be followed by the particles in following points:

to determine the value of the Stokes number, for particular value of density ratio s , from diagram in Fig. 1 for $\eta=0.99$

for particles with diameter D and for the fluid with viscosity ν , to calculate the maximum frequency of disturbances that can be followed by the particles. For water and air, it is possible to deduct from the diagram Fig. 4.

to check if the calculated frequency is higher than the maximum frequency that we want to measure. If the calculated frequency is lower it is possible to use the given type of the particle in case that the phase lag deducted from the diagram in Fig. 2 or 4 is of the order of ones of degrees or smaller. If the calculated frequency is lower than the maximum frequency that we want to measure it is recommended to use particles with smaller diameter or possibly the particles with lower value of specific density s .

In order to achieve the speed and integrity of the work it is necessary to introduce a diagram of dependence of the Stokes number on the frequency of disturbances for readily available seeding particles. This characteristic is plotted in diagrams in Fig. 4 which enable us to find quickly the searched frequency of disturbances in the flow for particular size of Stokes number and for the given particle. The usage of the suggested procedure at measuring in water and air is exemplified in the following paragraph.

In case that we measure in water at temperature of 20°C with particles with a mean diameter of 5 μm and specific density $s=1.1$ we can read from the diagram in Fig. 1 for $\eta=0.99$ the value of the Stokes number c . $NS=0.35$. The maximum frequency of disturbances which is measurable with given accuracy in water with such particle can be read from the diagram in Fig. 4 (eventually we can calculate it from the equation 4). The frequency that is followed by the particles with accuracy better than one percent and which was deducted from the diagram in Fig. 4 is 50 kHz. It is possible to consider this frequency as satisfactory for most cases of flow in water. For completeness' sake it is necessary to check the size of the phase lag. For value $NS=0.35$, the maximum phase lag with frequency of disturbances 40 kHz, $\beta=0.7^\circ$ can be read from the diagram in Fig. 2. It is possible to use the given particles in case that we assume the frequencies of disturbances in water lower than 50 kHz. Let's introduce the similar case for standard particles used at measuring in the air. Such particles are most frequently generated by fog generators and mean particle diameter value is c . 1 μm , specific density of particle/air is $s=670$. In this case, for $\eta=0.99$, s a d we can read the Stokes number $NS=17$ from the diagram in Fig. 3. The diagram in Fig. 5 allows us to determine, for the value NS and for the mean particle diameter 1 μm , the maximum frequency that can be followed by the particles i.e. 7 kHz. What remains to be checked is the size of the phase lag $\beta=10^\circ$, deducted from the diagram in Fig. 2. The determined maximum value of disturbance frequency that can be followed by the particles, i.e. 7 kHz, and the phase lag 10° are not the optimum values for measurement in the air during which the frequencies of the order of tens of kHz are to be expected. Consequently, if we want to observe the processes in the air whose frequency is higher than 7 kHz it is necessary to choose more suitable seeding particles. When choosing the more suitable seeding particles we can make use of a table 1 that contains the most frequent types of seeding particles and their features, and the relevant values of frequencies which can be followed by them. The table clearly shows us that when choosing the more suitable seeding particles the mean value of particles diameter and their specific density s are very important parameters. In general, the smaller the particles diameter and the more the specific density approaches one, the bigger the ability of particles to follow the flow field. If we accordingly use the same particles with diameter $d=0.3 \mu\text{m}$ then the maximum frequency for $NS=17$ read for such particles from diagram in Fig. 4 is 90 kHz.

4. The time response of the particle

If we neglect, in equation (1), all terms on the right side except the term expressing the drag force affecting the particle that moves in the flow field with velocity different from that of a liquid, then the equation (1) will change into the form of:

$$m \frac{du_p}{dt} = \frac{1}{2} C_D \frac{\pi d_p^2}{4} \rho_F (u_F - u_p) |u_F - u_p| \quad (8)$$

Where:	CD	drag coefficient of particle
	D	seeding particle diameter
	ρ_F	fluid density
	u_F	velocity of the fluid
	u_P	velocity of the particle
	m	particle mass
	du_p/dt	velocity gradient

It is a case of balance between an inertial force proportional to the mass of a particle and a drag force given by particle shape and size. By means of the equation (8) we can describe the situation when seeding particles are introduced into the flowing liquid whereas these particles have a different velocity than the fluid. Another example is the steady flow in a curved channel when due to the centrifugal acceleration the heavier particles can be moved from the original radius r at the entrance to the bigger radius $r + \Delta r$. The centrifugal acceleration can reach even the order of thousands of g by high velocities of the flow in the curved channel. In such a case it is necessary to verify the fault of the PIV measurement. If we introduce the Reynolds number of particle respecting the relative velocity of the particle in flowing fluid ($u-v$), and if the resulting Reynolds number calculated from the particle and fluid relative velocity is markedly smaller than one, it is possible to consider the flow around the particle to be creeping. The solution of equation (7) based on previous assumptions with constant flow velocity $u = \text{const.}$, and with zero initial velocity of the particle $v_0 = 0$ can be written down in following form:

$$u_p = u_F (1 - e^{-t/\tau_V}) \quad (9)$$

where τ_V is classified as time response of the particle:

$$\tau_V = \frac{\rho_P d_P^2}{18\mu_c} \quad (10)$$

The time response of the particle expresses the particles' ability to follow the liquid flow. It is the time interval during which the particle accelerates from zero velocity up to the value of c. 63.2 % of liquid

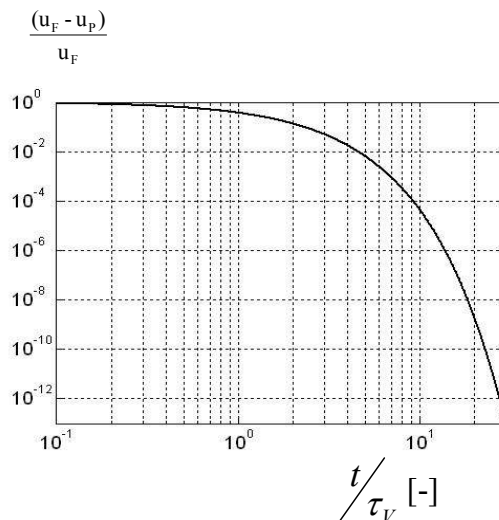


Fig. 3: The course of equalization of particle and liquid velocity in non-dimensional coordinates.

flow velocity. The response time of particle depends both on the particle size and material, and on viscosity of fluid that the particles move in. The response time of the same particles is different in environments with different viscosity. The time interval Δt during which the particle reaches

$uP=0.99uF$ at constant liquid velocity uF is equal to c. 4.5 multiple of the particle response time τ_V .

For time interval equal to 10 multiple of τ_V , the difference between the liquid and particle velocity is only 4.5 thousandth of the percent. In the diagram in Fig. 3 we can follow the difference between the particle and liquid velocity depending on the multiples of the particle response time. The advantage of such projection is the fact that it enables us to follow the particle and liquid speed equalization independently of the size of the response time of particle which is to be used in the experiment. The concrete time interval during which the speed equalization of both velocities takes place with required accuracy is possible to obtain easily by multiplying of the deducted value by the response time of particle we want to use in the measurement.

It is evident from above mentioned that the smaller the particle time response the bigger the particle's ability to follow the sudden changes in the flow. Let's assume again a harmonic motion of the particle when calculating the maximum frequency which can be followed by the particle with the help of the time response. The frequency of such motion is equal to:

$$f = \frac{\omega}{2\pi} \tag{11}$$

At calculating the maximum frequency it is necessary to determine the angular velocity ω . In diagram 3, as mentioned earlier, it occurs that for 4.5 multiple of the particle response time the difference between the particle and fluid velocity is smaller than one percent. If the angular velocity is equal to the reciprocal value of 4.5 multiple of the time response we can calculate the maximum frequency of disturbances that can be followed by the particles according to equation:

$$f_{MAX} = \frac{1}{9\pi\tau_V} \tag{12}$$

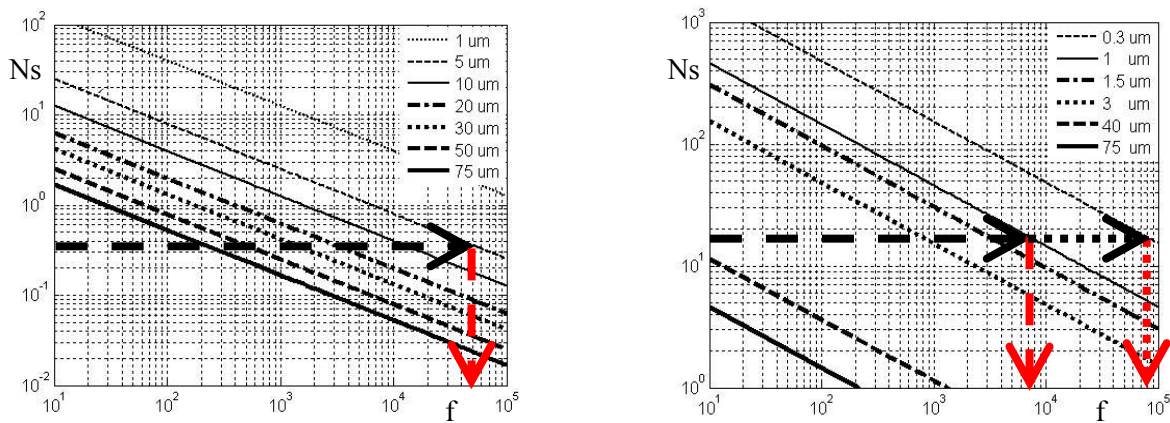


Fig.4: Dependence of Ns on dimensionless frequency for particles moving in water (A) and in air (B)

Tab 1: Parametres of particles used for measuring by the PIV method

Particles used for measuring in liquids				
Dynamic viscosity of water at 20 °C 1.002 10 ⁻³ [kgm-1s-1]				
Material of particle	Polyamide	Glass particles	Silvered glass particles	Fluorescent particles
Density [kgm-3]	1030	1100 [kgm-3]	1400 [kgm-3]	1500 [kgm-3]
Diameter [μm]	5	5	5	10
	10	10	10	30
	20	20	20	75
Response time of particle τ [μs]	1.42	1.5	1.9	8.32
	5.71	6.10	7.76	74.850
	22.84	24.4	31	467.81
fMAX - BBO	>100 kHz	50 kHz	12 kHz	2.3 kHz
	79 kHz	11 kHz	2.8 kHz	250 Hz
	18 Hz	2.6kHz	850 Hz	45 Hz
fMAX – τv	25 kHz	23 kHz	18 kHz	4.3 kHz
	6.2 kHz	5.8 kHz	4.6 kHz	470 Hz
	1.5 kHz	1.4 kHz	1.1 kHz	75 Hz
Particles used for measuring in liquids				
Dynamic viscosity of water at 20 °C 1.71 10 ⁻⁵ [kgm-1s-1]				
Material of particle	Oil	Water	Aluminium powder	Polystyrene microballs
Density [kgm-3]	800	1000	2700	30
Diameter [μm]	1	1	0.3	40
	1.5	1.5		100
	3	3		
Response time of particle τ [μs]	2.60	3.25	0.79	155.95
	5.85	7.31		714.75
	23.40	29.24		
fMAX - BBO	7 kHz	6 kHz	25 kHz	85 Hz
	3.2 kHz	2.7 kHz		15 Hz
	810 Hz	700 Hz		
fMAX – τv	13.6 kHz	10.8 kHz	44.8 kHz	226 Hz
	6 kHz	4.8 kHz		50 Hz
	1.5 kHz	1.2 kHz		

5. Conclusion

Based on the presented approaches it is possible to determine the maximum frequency of disturbances that can be followed by the concrete particles. The comparison of both methods is summarized in table 1 which contains the response times of individual particles as well as maximum frequencies based on BBO equation solution and based on the time response calculation. The comparison of both methods shows full correspondence between both approaches. From the results it is evident that if specific gravity of the particle and fluid approaches one, the maximum frequencies calculated by means of BBO equation are higher than the values determined by means of time response. On the contrary, at higher specific gravity the maximum frequency calculated by means of BBO equation is lower than value determined from time response. This behavior is given by the fact that the influence of particular BBO equation terms changes with changing particle and fluid density ratio. The measurement by the PIV method makes also use of different particles than those presented in table 1 with their maximum frequencies which is the reason why the paper proposes the method, for given particle type and given

fluid, with the help of which it is possible to easily and quickly determine the frequency to be followed by the particles with chosen accuracy.

6. Acknowledgment

This project has been supported by the MPO TA01010184

7. References

- Adrian Ronald, J. (1986) Image shifting technique to resolve directional ambiguity in double-pulsed velocimetry, *Optical society of America*.
- Astarita, T., G. Cardone. (2005) Analysis of Interpolation Schemes for Image Deformation Methods in PIV, *Experiments in Fluids* 38, 233-243, DOI 10.1007/S00348-004-0902-03.
- Basset, A. B. (1888) A Treatise on Hydrodynamics, *Deighton, Bell and Co.*, Cambridge.
- Bolinder, J. (1990) On the Accuracy of Digital Particle Image Velocimetry system, *Technical report*, ISSN 0282-1990.
- Byoung Jane K., Hyung Jim S. (2006) A Further Assessment of Interpolation schemes for Window Deformation in PIV, *Experiment in Fluids*, 499-511.
- Byoung Jae K., Chetan Swarup, Hyung Jin Sung, *Interpolation for Image Deformation in PIV*.
- Corsin, S., (1961) Lumely Appl. Csi. Res. A6 1961. 114.
- Crowe C., Sommerfeld M., Tsuji Y., *Multiphase Flows with Droplets and Particles*, CRC Press LLC Washington, D.C.
- Czarnecki, J., Dabros, T. (1980) Attenuation of the van der Waals Attraction Energy in the Particle/ Semi-Infinite. *Medium System due the Roughness of the Particle Surface*, J. Colloid Interface, 78, 25.
- Gui, L., S. T. Wereley. (2002) A Correlation-Based Continuous Window-Shift Technique to Reduce the Peak-Locking Effect in Digital PIV Image Evaluation, *Experimental in Fluids* 32, 506 – 517, Springer Verlag 2002, DOI 10.1007/S00348-001-0396-1.
- Gui L., Merzkirch W., Fri R., (2000) A Digital Mask Technique for Reducing the Bias Error of the Correlation-Based PIV Interrogation Algorithm, 30-35, *Experiments in Fluids*.
- Hart D. P., (1999) Super-Resolution PIV by Recursive Local-Correlation, *Journal of Visualization*, Vol 10.
- Hesham El-Batsh, (2001) Modeling Particle Deposition on Compressor and Turbine Blade Surfaces, *PhD Thesis*, Vienna University of Technology, Pohl gasse 8/1/3, A-1120 Vienna.
- Hinze, J. O., (1956) *Turbulence*, McGraw-Hill, New York.
- Hjelmfelt A. T., Mockros L. F., Motion of Discrete Particles in a Turbulent Fluid, *Appl. Sci. Res. Vol. 16*, 149-161.
- Liang, D.F., C.B. Jiang, Y.L. Li, (2002) A Combination Correlation-based Interrogation and Tracking Algorithm for Digital PIV evaluation. *Experiments in Fluids* 33, 684-695.
- Linken R., C. Poelma, J. Westerweel, (2003) Compensation for Spatial Effects for Non-Uniform Seeding in PIV Interrogation by Signal Relocation, *5th international Symposium on Particle Image Velocimetry*, Busan, Korea.
- Nobach H., Honkanen M., (2005) Two-Dimensional Gaussian Regression for Sub-Pixel Displacement Estimation in Particle Position Estimation in Particle tracking Velocimetry, *Experiments in Fluids* 38, 511-515.
- Raffel M., C. Willert, J. Kompenhans, (2007) *Particle Image Velocimetry*, Springer-Verlag, Second Edition, Berlin, ISBN 978-3-540-72307-3.
- Raffel, M., Ronneberger O., Kompenhans J., (1998) Advanced Evaluation Algorithms for Standart and dual Plane Particle Image Velocimetry, *Proc. 9th Intl. Symp. on Laser Techniques to Fluid Mechanics*, Lisbon (Portugal). 13–16 July.
- Saffman P., G., (1965) The Lift on Small Sphere in Slow Shear Flow, *J. Fluid Mech.* 22, 385.
- Scarano F., Riethmuler M., L., (2000) Advances in Iterative Multigrid PIV Image Processing, *Experiment in Fluids*, 851-860.
- Scarano F., Riethmuller M. L., (1999) Iterative Multigrid Approach in PIV Image Processing with Discrete Window Offset, *Experiment in Fluids* 26, 513-523.
- Scarano F., (2004) 2nd Derivatives Ccross-Correlation Based PIV Super-Resolution, *12th International Symposium on Applications of Laser Techniques to Fluid Mechanics*, Lisbon, Portugal.
- Sommerfeld M., (2000) Theoretical and Experimental Modeling of Particle Flows, *Von Karman Institute for Fluid Dynamics*, Lecture Series.

- Westerweel, J., Dabiri, D., and Gharib, M., (1997), The Effect of a Discrete Window offset on the Accuracy of Cross-Correlation Analysis of Digital PIV Recordings, *Experiment in Fluids* 23, 20-28.
- Westerweel J., (1997) Fundamentals of Digital Particle Image Velocimetry, *Measurement science and technology* 8, 1379-1392, UK.
- Westerweel J., (1993) Digital Particle Image Velocimetry - Theory and Application, *Delftse Universitaire Pers III, PhD Thesis*, Technische Universiteit Delft, ISBN 90-6275-881-9.
- Westerweel J., (2000) Theoretical Analysis of the Measurement Precision in Particle Image Velocimetry, *Experiments in Fluids* s3-s12, Springer - Verlag.
- Westerweel J., (2005) Analysis interrogation With Low Ppixel Resolution, *SPIE*, 624-635.